J2.7 A COMPARISON OF METHODS TO ESTIMATE THE DISSIPATION RATE IN A WIND TUNNEL CANOPY FLOW MODEL

W. Zhu, R. Van Hout and J. Katz*
The Johns Hopkins University, Baltimore, Maryland

ABSTRACT

PIV data obtained in a wind tunnel canopy flow model is used for comparing three methods for estimating the dissipation rate. The spatial resolution of the measurements is 1.7-2.5 times the Kolmogorov scale. The first method is based on a curve fitting to the energy spectrum in the inertial subrange. The second consists of calculating the SGS energy flux; and the third is based on direct measurements of instantaneous velocity gradients, i.e. it measures the overall dissipation rate. The SGS energy flux is scale dependent, decreasing with decreasing scale in the dissipation range. The spectral estimate is twice the SGS energy flux near canopy height, but this ratio decreases at higher elevations. The curve-fitted estimate is larger than the overall dissipation in the vicinity of canopy height and smaller than it at higher elevations, but the difference between them is in the 5% to 30% range. These trends agree with Finnigan's (2000) conclusion that a -5/3 spectral fit overestimates the cascading energy flux.

1. INTRODUCTION

Dissipation rate is the only term depleting energy in the evolution equation for turbulence kinetic energy. The magnitude of dissipation is commonly estimated by curve fitting to the energy spectrum in the inertial range, using the Kolmogorov spectrum (Brunet et al. 1994; Raupach et al. 1986; Shaw et al. 1974; Pope, 2000). However, in canopy flow, the spectrum is modified due to interaction of canopy elements with the large scale turbulence, which bypasses the cascading process. Finnigan (2000) proposes a modified Kolmogorov theory that leads to a different shape of energy spectrum. His analysis leads him to the conclusion that the cascading part of energy dissipation, estimated from a -5/3 fit to the energy spectra, over estimate the real value by 2.5-3 times in a forest canopy and by about one third in a wind tunnel model.

As discussed in Finnigan (2000), the bypass depletes energy from the mean flow and large-scale turbulence and transfers it to small scales directly. Thus, the cascading flux represents only part of the total dissipation. In this paper we use 2-D Particle Image Velocimetry (PIV) data obtained in a canopy flow model to compare the spectral fit to two other methods for estimating the cascading energy flux and dissipation rate. The spatial resolution, 1.7-2.5 times the Kolmogorov scale, enables us to estimate dissipation from the instantaneous velocity gradients. Spatial filtering of the data enables us to calculate the subgrid scale (SGS) energy flux at different scales. We show that for the present test condition, where the canopy element size falls within the dissipation rate, the spectral and direct estimates of overall dissipation are close, but the spectral fit is even larger than the overall dissipation in the vicinity of canopy height. The SGS energy flux in the inertial range is about 40% of the overall dissipation within the canopy and 60% above it.

2. EXPERIMENTAL SETUP

PIV measurements of canopy flow have been performed in the Corrsin wind tunnel at The Johns Hopkins University. The experimental setup is presented in Fig. 1a. The wind tunnel has a 10 m long test section with a cross section of 1.2x0.91 m^2 and is equipped with an active grid to enhance the turbulence intensity. Using a mean shear generator, consisting of screens with varying mesh size, the mean velocity profile at the measuring position is adjusted to match the profile measured in a corn field (van Hout et al., 2005). As shown in Fig. 1b, the model canopy consists of an array of 30 cm long wooden sticks with diameter of 3.2 mm. They are inserted in 5 cm thick styrofoam. Thus the height of canopy elements is h = 25 cm. Further details can be found in Zhu et al. (2006).

For all the measurements, the mean velocity at canopy height is U_h = 3.17 m s^{-1}. The PIV field of view is 4.86x4.86 cm^2, and the sample streamwise-vertical plane is located at the centerline of the wind tunnel, between two rows of canopy elements. We remove one row of sticks, which is marked by x in Fig. 1b, in order to observe the flow in the sample plane. The PIV data have been processed using 32x32 pixel interrogation windows with 50% overlap. The uncertainty in instantaneous measurements is about 0.2 pixels, i.e. 0.05 ms^{-1} (Roth et al., 1999; 2001). Fig. 2 shows a sample of an instantaneous velocity map around canopy height.

* *Corresponding author address:* Joseph Katz, The Johns Hopkins University, Department of Mechanical Engineering, 3400 N. Charles Street, Baltimore, MD 21218; e-mail: katz@poseidon.me.jhu.edu

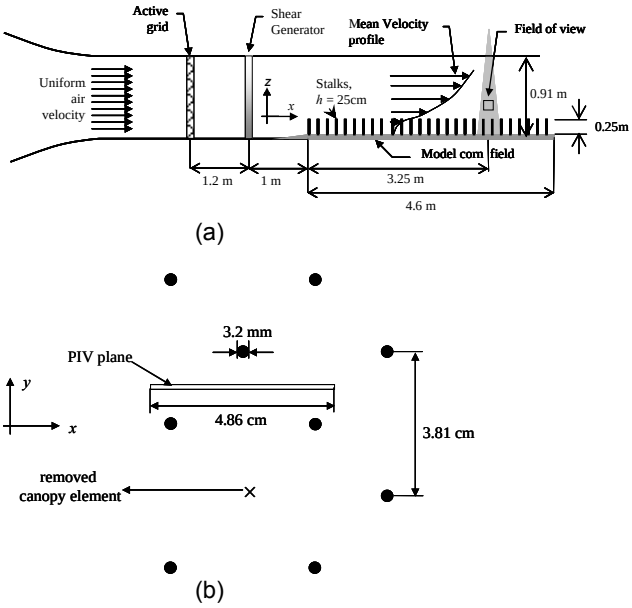

Fig. 1 (a) Wind tunnel model canopy and experiment setup (not to scale); (b) Configuration of model canopy.

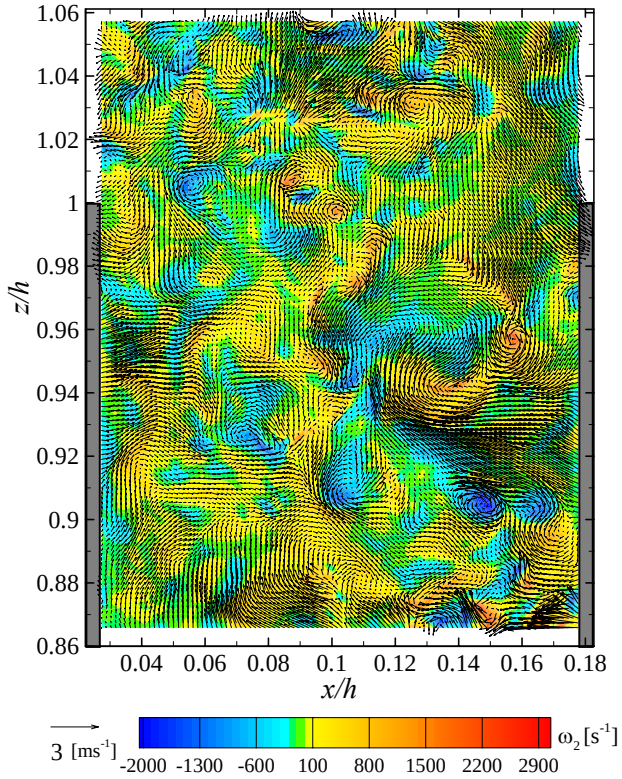

Fig. 2 Vector map of an instantaneous velocity field superimposed on the vorticity distribution. The instantaneous spatial mean velocity, $(5.61,-1.21)$ [ms^{-1}], is subtracted to highlight the flow structure.

In presenting the results, $x_1 = x$, $x_2 = y$, $x_3 = z$, are the streamwise, lateral, and wall normal direction respectively; and u_1, u_2, u_3 are the corresponding instantaneous velocity components. The fluctuating velocity components are represented by u_1', u_2', u_3'. Spatial averages using a box filter of scale Δ are denoted by tilde, $(\tilde{..})$.

3. ENERGY FLUX AND DISSIPATION RATE ESTIMATE

3.1 *Spectral Fitting*

Fig. 3 compares κ_1 compensated streamwise energy spectra of the horizontal velocity component, $\kappa_1 E_{11}(\kappa_1)$, below and above canopy height. The results are normalized with spectrally estimated cascading part of the dissipation rate and the Kolmogorov scale. The cascading flux, ε, is estimated by fitting a -2/3 line to the κ_1 compensated spectra, assuming that (Pope, 2000)

$$E_{11}(\kappa_1) = \tfrac{18}{55} 1.6 \varepsilon^{2/3} \kappa_1^{-5/3} \quad (1)$$

The Kolmogorov scale is estimated from:

$$\eta = (\upsilon^3/\varepsilon)^{1/4} \quad (2)$$

Estimated values of ε and η at several elevations are provided in Table 1. Based on the results, the thickness of canopy element is ~20η and is marked by an arrow in Fig. 3. The spectra are calculated using fast Fourier transforms. To reduce the effect of the finite data sets, we remove the mean and apply linear detrending with zero padding. No windowing function is used. Details can be found in Doron et al. (2001) and Nimmo Smith et al. (2005). The spectra presented here are calculated separately for each horizontal line (containing 128 vectors) in the 2-D vector maps, ensemble averaged, and then averaged over the 11 central lines of the velocity distributions.

In Fig. 3, above the canopy, the normalized spectra collapse. The same trend persists at other elevations and for the vertical component (not shown). Below the canopy, the energy decreases at low wavenumbers and increases at high wavenumbers with decreasing elevation. This trend has been measured before by Raupach et al. (1986). Some of the increase in energy at small scales is caused by noise, but not all of it. Some is associated with the bypass mechanism caused by interaction of canopy elements with mean flow and large scale eddies. Indeed the scale of canopy element, falls in the wavenumber range with the highest deviation of the spectra below canopy height from those at *z/h* > 1.

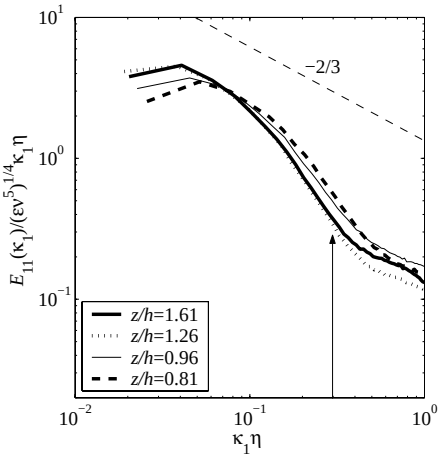

Fig. 3 Normalized $\kappa_1 E_{11}(\kappa_1)$ below and above the canopy. Arrow indicates scale of canopy elements.

Table 1 The Kolmogorov scale and a comparison of dissipation rates estimated by a $-5/3$ line to the energy spectra, ε, to direct calculation, ε^d, and to SGS energy flux, ε^{SGS}, at Δ~70η.

z/h	η[μm]	ε[m^2 s^{-3}]	ε^d[m^2 s^{-3}]	ε^{SGS}[m^2 s^{-3}]
2.13	215	1.58	2.33	1.11
1.96	192	2.48	3.16	1.60
1.78	178	3.36	3.94	2.47
1.61	157	5.50	4.80	2.95
1.43	151	6.51	5.20	3.02
1.26	148	7.06	5.36	3.02
1.10	150	6.74	5.78	3.34
0.96	137	9.66	9.17	4.42
0.81	156	5.75	6.59	3.56

Focusing on the small scale turbulence, in Fig. 4a and b, we also show "dissipation spectra", i.e. $\kappa_1^2 E_{11}(\kappa_1)$ and $\kappa_1^2 E_{33}(\kappa_1)$, respectively, and compare them to universal spectra available in Gargett et al. (1984) and Luznik et al. (2006). The dissipation spectra are presented in linear scales, highlighting small scale phenomena. The measured spectra are normalized by finding the values of ε that best fit the universal dissipation spectra. These values deviate from those estimated from the energy spectra by 5-24%. As is evident, our data clearly extend to scales that are significantly smaller than the peak in dissipation. At high wavenumbers, the spectra turn upward, in part but not only due to effects of noise. To show that, note $\kappa_1^2 E_{11}(\kappa_1) > \kappa_1^2 E_{33}(\kappa_1)$, as one would expect for small turbulent eddies generated in the wake of canopy elements. Also, both spectra start deviating substantially from the universal spectra at $\kappa_1\eta$ = 0.2~0.3, i.e. at scales comparable to those of the canopy elements. This scale corresponds to 8 vector spacings, well above the range where noise has substantial effect on our typical PIV based spectra of turbulent flows (e.g. Chen et al. 2005, Nimmo Smith et al. 2005). Finally, for the field data obtained recently within a corn canopy (van Hout et al. 2006), the small scale energy of the horizontal velocity component is higher than that of the vertical component, consistent with the present trends. Thus, part of the abrupt deviation from the universal spectra is caused by interactions with canopy elements. The largest small scale deviation occurs close to the canopy height. Well above the canopy the deviation occurs at higher wave numbers.

At low wavenumbers the normalized dissipation spectra follow the universal curves quite closely. However, close to canopy height, in the range 0.15< $\kappa_1\eta$ <0.3, $\kappa_1^2 E_{33}(\kappa_1)$ falls slightly below the universal values, whereas $\kappa_1^2 E_{11}(\kappa_1)$ does not. We have seen the same trends in the corn field data (van Hout et al. 2006). Clearly the turbulence in the vicinity of the canopy is anisotropic at all scales, consistent with Finnigan (2000) and Raupach et al. (1986).

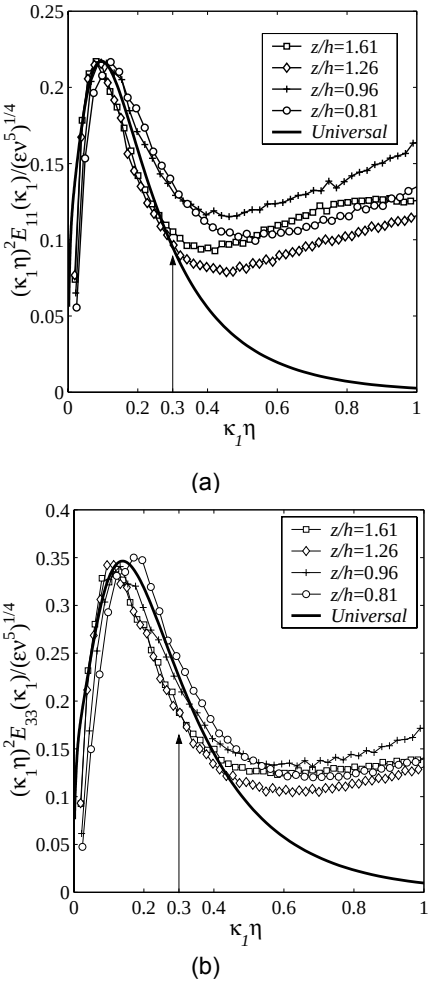

Fig. 4 (a) Dissipation spectra plotted with universal dissipation spectra from Gargett et al. (1984), $\kappa_1^2 E_{11}(\kappa_1)$ component, (b) $\kappa_1^2 E_{33}(\kappa_1)$ component. Arrow indicates scale of canopy elements.

3.2 *Directly Estimated Dissipation Rate*

By definition, the dissipation rate is

$$\varepsilon^d = 2\nu\overline{s_{ij}s_{ij}} \tag{3}$$

where s_{ij} is the fluctuating strain rate. Since we only have in-plane velocity components, we multiply the in-plane contribution by 15/7, which for isotropic turbulence would give the exact value (Fincham et al. 1996). The resulting "direct" estimate is:

$$\varepsilon^d = \tfrac{15}{7}\nu\left[2\overline{\left(\frac{\partial u_1'}{\partial x}\right)^2} + 2\overline{\left(\frac{\partial u_3'}{\partial z}\right)^2} + \overline{\left(\frac{\partial u_1'}{\partial z}\right)^2} + \overline{\left(\frac{\partial u_3'}{\partial x}\right)^2} + 2\overline{\left(\frac{\partial u_1'}{\partial z}\frac{\partial u_3'}{\partial x}\right)}\right] \tag{4}$$

Since our vector spacings, 1.7-2.5η, are slightly under resolved for direct measurements of velocity gradients, we are under estimating the dissipation rate, but not substantially. These estimates provide the total dissipation, not only the cascading part. The results are compared to the spectral fits in Table 1. As is evident, the spectrally calculated cascading energy flux deviate from the directly estimated dissipation rates by 5-30%, with $\varepsilon^d > \varepsilon$ well above the canopy and at *z/h* = 0.81.

3.3 *Subgrid Energy Flux*

The second approach for estimating the energy flux from large to small scale is to calculate the SGS energy flux or SGS dissipation, ε^{SGS}. By spatially filtering the PIV data at different scales, Δ, ε^{SGS} is the energy flux from the flow at scales larger than Δ to subgrid scales, which are smaller than Δ (Liu et al. 1994, 1999). For homogenous isotropic turbulence, and filter scale falling in the inertial subrange, ε^{SGS} is almost equal to ε (Pope, 2000). The in-plane contribution to the SGS dissipation, $\varepsilon_{2D}^{SGS}(\Delta)$, is:

$$\varepsilon_{2D}^{SGS}(\Delta) = -(\tau_{11}\tilde{S}_{11} + \tau_{33}\tilde{S}_{33}) - 2\tau_{13}\tilde{S}_{13} \tag{5}$$

where $\tau_{ij} = \widetilde{u_i u_j} - \tilde{u}_i\tilde{u}_j$ is the SGS stress tensor and $\tilde{S}_{ij} = \frac{1}{2}(\partial\tilde{u}_i/\partial x_j + \partial\tilde{u}_j/\partial x_i)$ is the resolved (filtered) strain-rate tensor (Liu et al. 1999). The same factor, 15/7, used for direct estimate of dissipation from 2-D PIV data is also applicable to the SGS dissipation, i.e. for homogeneous isotropic turbulence:

$$\varepsilon^{SGS}(\Delta) \cong 15/7\,\varepsilon_{2D}^{SGS}(\Delta) \tag{6}$$

Note that since the resolved scales include the mean flow, the SGS flux includes all the energy flux from resolved to sub-grid scales. Fig. 5 shows the SGS energy flux normalized by ε^d as a function of filter size, which ranges between 5–40 vector spacings, corresponding to approximately 10η to 100η. For all elevations above canopy height, the SGS flux decreases with decreasing filter scale, as expected for the dissipation range, but the curves flatten in scales falling within the inertial range, also consistent with expectation. Trends of the two elevations below canopy height are distinctly different from those measured at *z/h* > 1. Above the canopy, ε^{SGS} reaches 60% of ε^d, while below the canopy, ε^{SGS} is only 40–50% of ε^d (Table 1). Furthermore, below canopy height, the slope is small for Δ/η>20, the size of canopy elements. Thus, in spite of being within the dissipation range, the SGS energy flux does not decrease significantly with decreasing scale. Since some of the energy is dissipated in this range, there must be another source that replenishes it. Does the bypass mechanism cause this effect?

4. DISCUSSION AND CONCLUSIONS

The values of $\varepsilon^{SGS}/\varepsilon$ for Δ~70η are shown in Fig.6. Well above the canopy, $\varepsilon^{SGS}/\varepsilon$ exceeds 0.7, i.e. the difference between them is quite small, but close to canopy height, this ratio decreases to the 43% - 53% range. Clearly, the discrepancy between the spectral fit and measured SGS flux increases near canopy height, consistent with Finnigan's (2000) conclusion that a -5/3 spectral fit overestimates the cascading energy flux. "Deep" within the canopy the ratio increases again, mostly due to a sharp decrease in ε.

The ratio $\varepsilon/\varepsilon^d$, shown in Fig. 7, exceeds 1 in the $0.96 \le z/h \le 1.61$ range, i.e. the spectral estimate is even larger than the overall dissipation rate. This ratio is significantly less than 1 well above the canopy. This trend also confirms that the extent that the spectral estimate of dissipation over predicts the energy flux increases significantly in the vicinity of canopy height, again consistent with Finnigan's (2000) conclusions.

To recapitulate, the spectrally estimated cascading energy flux is close in magnitude to the overall dissipation estimated directly from velocity gradients at slightly under resolved small scales. However, near canopy height ε is even larger than ε^d. The spectral estimate is also about twice the SGS energy flux just above and below canopy height. Far from the canopy ε is only 40% higher than ε^{SGS}. The ratio $\varepsilon^{SGS}/\varepsilon^d$ is scale dependent, reaching 0.6 for filter scale within the inertial range but decreasing substantially in the dissipation range. The variations of ε^{SGS} with scale are smaller within the canopy except for scales comparable to those of canopy elements.

ACKNOWLEDGMENT:

This research has been funded by the Bio-Complexity Program of the National Science Foundation, under grant No. BES 0119903. The authors would also like to thank H.S. Kang and C. Meneveau for their support and advice during the wind tunnel measurements.

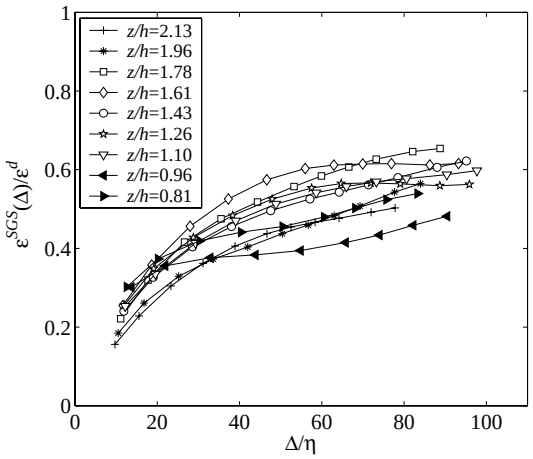

Fig. 5 The ratio of subgrid scale energy flux to directly estimated dissipation rate.

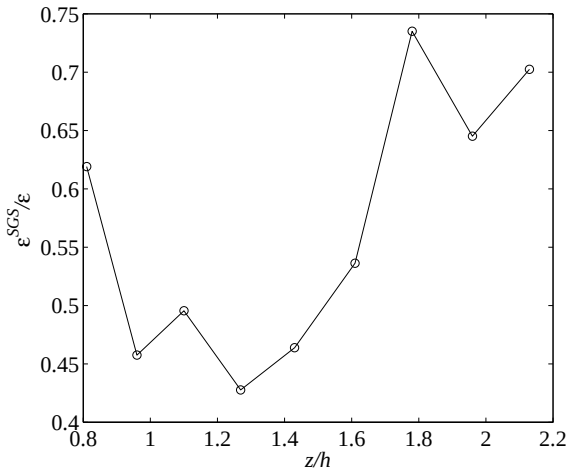

Fig. 6 The ratio of SGS energy flux ($\Delta \sim 70\eta$) to spectrally estimated energy flux.

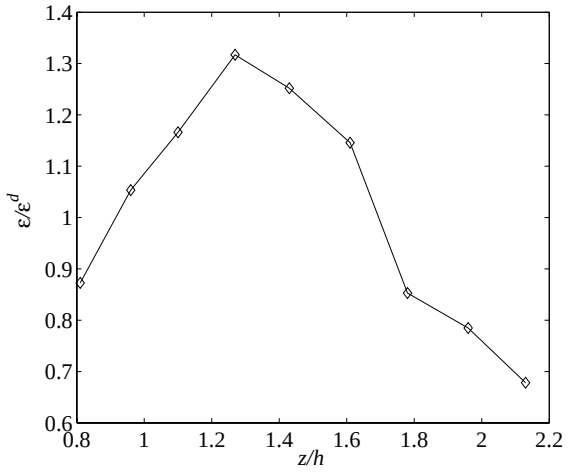

Fig. 7 The ratio of spectrally estimated energy flux to directly estimated dissipation rate.

REFERENCES:

Brunet, Y., Finnigan, J. J., and M. R. Raupach, 1994: A wind tunnel study of air flow in waving wheat: single point velocity statistics. *Bound.-Layer Meteor.*, **70**, 95-132.

Fincham, A. M., Maxworthy, T., and G. R. Spedding, 1996: Energy dissipation and vortex structure in freely decaying, stratified grid turbulence. *Dynam. Atmos. Oceans*, **23,** 155-169.

Finnigan, J. J.: 2000, 'Turbulence in plant canopies', *Ann. Rev. Fluid Mech*. **32**, 519-571.

Gargett, A. E., Osborn T. R., and P. W., Nasmyth, 1984: Local isotropy and the decay of turbulence in a stratified fluid. *J. Fluid Mech.*, **144**, 231-280.

Liu, S., Meneveau, C., and J. Katz, 1994: On the properties of similarity subgrid-scale models as deduced from measurements in a turbulent jet. *J. Fluid Mech.*, **275**, 83-119.

Liu, S., Katz, J, and C. Meneveau, 1999: Evolution and modeling of subgrid scales during rapid straining of turbulence. *J. Fluid Mech.*, **387**, 281-320.

Luznik, L., Gurka, R., Nimmo Smith, W. A. M., Zhu, W., Katz, J. and T. R. Osborn 2005: Distribution of energy spectra, Reynolds stresses, turbulence production and dissipation in a tidally driven bottom boundary layer. Submitted to *J. Phys. Oceanogr.*

Nimmo Smith, W. A. M., Katz, J., and T. R. Osborn, 2005: On the structure of turbulence in the bottom boundary layer of the coastal ocean. *J. Phys. Oceanogr.*, **35**, 72-93.

Pope, S. B.: 2000, *Turbulent flows*, Cambridge University Press, 771 pp.

Raupach, M. R., Coppin, P. A., and Legg, B. J.: 1986, 'Experiments on scalar dispersion within a model plant canopy, Part I: the turbulence structure', *Boundary-Layer Meteorol*. **35**, 21-52.

Roth, G. I., and Katz, J.: 1999, 'Parallel truncated multiplication and other methods for improving the speed and accuracy of PIV calculations', *Proceedings of the 3rd ASME/JSME Joint Fluids Engineering Conference*, July 18-23, San Francisco, CA.

Roth, G. I. and Katz, J.: 2001, 'Five techniques for increasing the speed and accuracy of PIV interrogation', *Meas. Sci. Technol.* **16**, 1568-1579.

Shaw, R. H., Silversides, R. H., and G. W. Thurtell, 1974a: Some observations of turbulence and turbulent transport within and above plant canopies. *Bound.-Layer Meteor.*, **5**, 429-449.

van Hout, R., Zhu, W., Luznik, L., Katz, J., Kleissl, J., and Parlange, M.: 2006, 'PIV measurements in the atmospheric boundary layer within and above a mature corn canopy; Part A: Statistics and small scale isotropy', Submitted to *J. Atmos. Sci*.

Zhu, W., van Hout, R., Luznik, L., Kang, H. S., Katz, J., and Meneveau, C.: 2006, 'A comparison of PIV measurements of canopy turbulence performed in the field and in a wind tunnel model', Submitted to *Exp. Fluids*.